

# Hydrogen Sensing and Sensitivity of Palladium-Decorated Single-Walled Carbon Nanotubes with Defects

Vaikunth R. Khalap, Tatyana Sheps, Alexander A. Kane, and Philip G. Collins\*

Department of Physics and Astronomy, University of California, Irvine, California 92697

**ABSTRACT** Individual single-walled carbon nanotubes (SWCNTs) become sensitive to H<sub>2</sub> gas when their surfaces are decorated with Pd metal, and previous reports measure typical chemoresistive increases to be approximately 2-fold. Here, thousand-fold increases in resistance are demonstrated in the specific case where a Pd cluster decorates a SWCNT sidewall defect site. Measurements on single SWCNTs, performed both before and after defect incorporation, prove that defects have extraordinary consequences on the chemoresistive response, especially in the case of SWCNTs with metallic band structure. Undecorated defects do not contribute to H<sub>2</sub> chemosensitivity, indicating that this amplification is due to a specific but complex interdependence between a defect site's electronic transmission and the chemistry of the defect–Pd–H<sub>2</sub> system. Dosage experiments suggest a primary role is played by spillover of atomic H onto the defect site.

**KEYWORDS** Carbon nanotube, hydrogen sensor, defect

Single-walled carbon nanotubes (SWCNTs) are wires with easily perturbed, one-dimensional conduction channels and extremely large ratios of surface area to volume. These properties make them attractive candidates for applications in gas and chemical sensing. In practice, though, pristine SWCNTs respond to an impractically broad range of common gases and liquids, and improving the selectivity and dynamic range of these responses remains an ongoing research challenge.<sup>1</sup> Some of the most dramatic improvements in prototype sensors have employed SWCNTs with modified surface chemistries, a technique first proven using SWCNT devices decorated with Pd clusters.<sup>2</sup> In 2001, Kong et al. showed that an isolated semiconducting SWCNT coated with discontinuous Pd would decrease electrical conductance by as much as 50% when dosed with H<sub>2</sub> gas (4–400 ppm in air), even though a pristine SWCNT has no such intrinsic response to H<sub>2</sub>. This result has been widely reproduced, as discussed in the recent review by Sun and Sun,<sup>3</sup> though subsequent research has focused on SWCNT films due to their ease of fabrication and perceived reliability benefits. Indeed, Pd-decorated SWCNT films became the first commercially available, nanotube-based chemical sensors,<sup>4</sup> but an understanding of the responsible sensing mechanisms has languished in the move to exploit this phenomenon.

Upon revisiting experiments on individual, isolated SWCNTs, we find that the presence or absence of point defects tremendously affects the observable H<sub>2</sub> response. A point defect provides a scattering center that can completely

determine the conductance of a SWCNT device,<sup>5</sup> and when it is decorated by Pd, the H<sub>2</sub> response amplifies this effect. Under conditions that reproduce the 50% drop in conductance on defect-free SWCNTs, we observe thousand-fold decreases in a SWCNT having a single defect. Previous work on SWCNT films damaged by sputtering inferred similar amplification from defects,<sup>6,7</sup> but here we demonstrate the magnitude of the effect by measuring single SWCNTs before and after defect incorporation. The results are of particular import for controlling and tailoring the response of SWCNT film devices, which contain various types of disorder including defects.<sup>8</sup>

**Experimental Methods.** Experimental samples are obtained by chemical vapor deposition (CVD) growth of isolated, small diameter (1.1 nm) SWCNTs on a thermally oxidized, p<sup>++</sup> Si substrate.<sup>9</sup> A 250 nm SiO<sub>2</sub> dielectric layer separates the SWCNTs from the Si in a backgated, field-effect transistor configuration. Contact electrodes of either Ti or Pd metal are defined on top of the SWCNTs on a 4.5 μm pitch by standard photolithographic techniques and e-beam deposition. In the case of Pd electrodes, 0.8 nm of Ti is initially deposited as an adhesion promoter. A final step in the fabrication is a brief anneal in air to 300 °C.

Following fabrication, individual SWCNTs are categorized as semiconducting or metallic (s-SWCNT or m-SWCNT, respectively) based on measurements of source–drain conductance  $G$  versus backgate voltage  $V_g$ . Defect-free s-SWCNTs have p-type  $G(V_g)$  curves with a monotonic modulation of at least 99%.  $G(V_g)$  curves with  $\leq 20\%$  modulation identify m-SWCNTs, and these make up a substantial fraction of the devices in this diameter range. Unless noted otherwise, all measurements are performed using a source–drain bias of 100 mV.

\* Corresponding author, collinsp@uci.edu.

Received for review: 10/28/2009

Published on Web: 02/15/2010



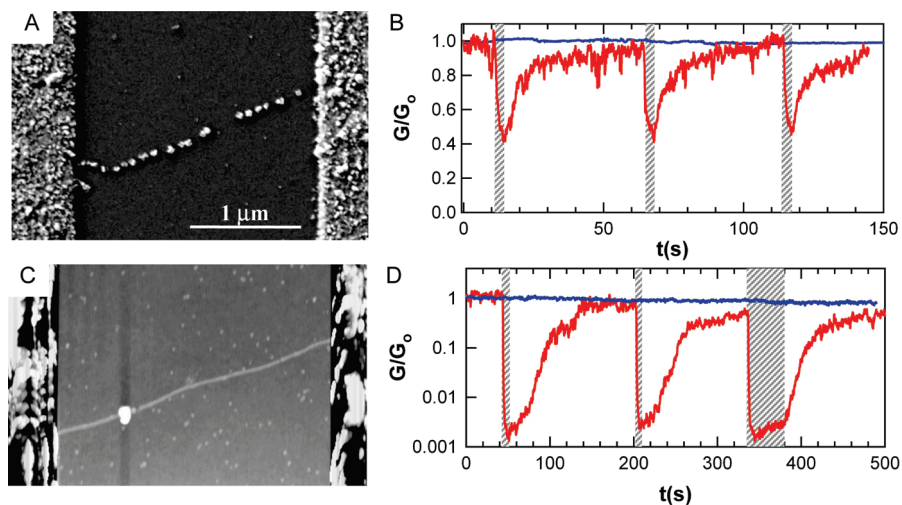


FIGURE 1. (A) Electron micrograph of a defect-free, *s*-SWCNT device with random Pd decorations all along its length. (B) Response of the device to pulses of H<sub>2</sub> in air, before (blue) and after (red) the Pd deposition. Note that despite using Pd metal for the contact electrodes, no response is observed without additional Pd decoration. (C) Atomic force topography image of a second SWCNT following the production of a point defect and selective decoration of the site with Pd. (D) Response of the defective device, before (blue) and after (red) Pd deposition, plotted on semilogarithmic axes to show the nearly thousand-fold response. *G* becomes very small in H<sub>2</sub> but remains measurably nonzero. In (B) and (D), the H<sub>2</sub> test exposures have similar but nonidentical timing that are depicted as gray hatched stripes; the four data sets are aligned for straightforward comparison.

After the SWCNTs are sorted, a portion of the devices are tested in their as-fabricated state, but most of the devices are electrochemically modified using three techniques. The first technique consists of nonselective electrodeposition of Pd nanoparticles from a PdCl<sub>2</sub> solution (0.1 mM PdCl<sub>2</sub> in 0.1 M HCl;  $V_{we} = -0.75$  V vs Pt). With 5 s deposition times, SWCNTs become dilutely coated with Pd particles up to 20 nm in diameter (Figure 1A). In the second technique, a more delicate, “selective electrodeposition” can be used to nucleate Pd nanoparticles on SWCNT defect sites without depositing metal on pristine regions.<sup>10</sup> Selective electrodeposition is achieved with the same electrolyte solution but using a tripotential method ( $V_{we} = -0.70$  for 10 ms, followed by  $V_{we} = -0.50$  V for 5 s) described previously for Ni deposition.<sup>10</sup> In this process, SWCNT defects are decorated by monodisperse, 20 nm Pd particles; SWCNTs without defects are unaffected (Figure 1C). Finally, a third experimental technique involves electrochemical oxidation to deliberately introduce SWCNT defects. In the point-functionalization method described previously,<sup>5</sup> defect creation is limited to single sites by monitoring *G* during oxidation, and by running the oxidation at threshold conditions (0.1 M HCl;  $V_{we} = +0.90$  V) where stochastic events are well separated in time. In all, approximately 40 individual SWCNT devices have been tested in this study, including *s*-SWCNTs and *m*-SWCNTs with different combinations of intentional oxidation and Pd decoration.

In all three electrochemical processes, extensive rinsing in deionized H<sub>2</sub>O is necessary to minimize surface contamination. In order to protect the contact electrodes and contact–SWCNT interfaces, and to restrict any modifications to the SWCNT sidewall, e-beam lithography of PMMA was used to expose only a short (~1 μm) segment of a SWCNT

to the chemical environment. In all three cases, this exposed SWCNT segment serves as a working electrode, and Pt counter and pseudoreference electrodes control the electrochemical potential  $V_{we}$  between an electrolyte and the SWCNT sidewall. We note that PMMA is permeable to the H<sub>2</sub> used in subsequent sensor testing, but not generally to the Pd<sup>+</sup> or Cl<sup>-</sup> ions used in these preparatory processes.

Preliminary chemoresistance responses are identified by measuring *G* in air while briefly dosing a device surface with pure H<sub>2</sub> gas. Devices exhibiting noticeable responses are transferred to a variable temperature vacuum system equipped with a bleed valve and a capacitance manometer (BOC Edwards 600G) for more accurate pressure measurements. To compensate for poor H<sub>2</sub> pumping speeds, evacuation was assisted by multiple cycles of purging. Similar to previous works on this topic,<sup>2,3,11,12</sup> substantial differences are observed between purge gases of dry N<sub>2</sub> and ambient air.

**Results and Discussion. a. Pristine, Defect-Free SWCNTs.** Individual, defect-free *m*-SWCNTs and *s*-SWCNTs show no appreciable changes in conductance *G* to any concentration of H<sub>2</sub> gas. The use of Ti or Pd connective electrodes, and the presence or absence of protective PMMA, did not result in any noticeable differences that could be attributed to the metal–SWCNT interfaces. While it is not surprising for *m*-SWCNTs to lack sensitivity, one might expect the Schottky barriers contacting *s*-SWCNTs<sup>15</sup> to be more sensitive to gases. In particular, Pd-contacted *s*-SWCNTs might exhibit substantial changes due to phase transitions between Pd and PdH<sub>x</sub> at the electrode interfaces.<sup>14</sup> No such changes are observed for H<sub>2</sub> dosing experiments performed at negative gate voltages  $V_g < 0$ , and a representative example is depicted in Figure 1B. Small

changes in  $G$  may in fact occur along the sidewall, but be masked by other, conductance-limiting mechanisms like the Schottky barriers. Substantial contact resistances on the order of 0.1–1 M $\Omega$  are typical for small-diameter SWCNT devices, even when contacted by Pd.<sup>15–17</sup>

After initial testing of the pristine devices, small Pd clusters were randomly nucleated on the SWCNTs by electrodeposition. Pd deposition increases  $G$  by 0–20% and reduces the effectiveness of the backgate electrode, two reasonable consequences of a discontinuous metal coating. Small deposition overpotentials minimized the likelihood of electrochemical modification of the SWCNT sidewalls, which would otherwise be accompanied by substantial decreases in  $G$ .

Figure 1B shows the time-varying conductance response  $G/G_0$  of a typical, Pd-decorated s-SWCNT device and compares it to that of an undecorated device. As reported by others,<sup>2,3</sup> the Pd decorations cause a H<sub>2</sub> sensitivity manifested by an immediate and rapid decrease of about  $\Delta G/G_0 = -60\%$ . These decreases are reversible and can be cycled multiple times, though recovery often requires 10–100 s for each cycle. Fitting portions of the curves to exponentials of the form  $e^{-t/\tau}$  give an average response time  $\tau = 1.0$  s and a recovery time  $\tau = 20$  s when devices are probed in air with pulses of H<sub>2</sub> gas. From the control measurement shown, it is clear that the Pd decorations, and not the Pd contact electrodes, are responsible for the effect. The mechanism proposed for this effect has generally been carrier scattering caused by local depletion around the Pd decoration.<sup>18</sup>

Unlike s-SWCNTs, m-SWCNTs do not respond to H<sub>2</sub> exposures in air, whether or not they are decorated with Pd. Under vacuum, m-SWCNTs do exhibit substantial, temporary increases in device noise, but not in the average value of  $G$ . This noise might be wholly due to the activation of charge traps in the underlying SiO<sub>2</sub> substrate as it is exposed to atomic, reactive H atoms dissociated by the Pd clusters.

**b. SWCNTs with Defects.** SWCNTs with Pd-decorated defects exhibit dramatically stronger responses to H<sub>2</sub> gas. Unlike the case described above, m-SWCNTs and s-SWCNTs both exhibit almost identical responses, and both become nearly insulating in H<sub>2</sub> when they contain Pd-decorated defects. To demonstrate this conclusion, defect-free SWCNTs were first measured as described above. Next, single defects were introduced by the point functionalization method.<sup>5</sup> Third, Pd was selectively deposited using tripotential, selective electrodeposition.<sup>10</sup> H<sub>2</sub> testing was performed on the defective devices before and after Pd decoration in order to separate any chemosensitivity of the SWCNT defect itself from the response of the defect–Pd complex.

Figure 1D shows the results of H<sub>2</sub> testing in air on a typical s-SWCNT device with a defect site. After defect introduction but before Pd decoration, the device is insensitive to H<sub>2</sub> exposure. After decoration,  $G/G_0$  decreases nearly 3 orders of magnitude in response to H<sub>2</sub> dosing. Similar amplification has been observed on every SWCNT device prepared in this

manner, including nine s-SWCNT and seven m-SWCNT devices investigated in detail during the course of this study. Even though the  $G/G_0$  response is exaggerated in the defective devices compared to the defect-free case, the characteristic timings  $\tau$  are very similar between Figure 1B and Figure 1D. As before, multiple H<sub>2</sub> cycles do not degrade the response.

In the presence of defects, m-SWCNTs and s-SWCNTs no longer have any difference in their H<sub>2</sub> responses. Both types of devices become equally sensitive to H<sub>2</sub> when defects are present. This result indicates that the underlying SWCNT band structure no longer plays any significant role in the amplified device response. Instead, we conclude that the response is predominantly due to scattering at the defect site. The addition of defects to a pristine SWCNT typically decreases the device conductance, with the entire effect concentrated at the defect site.<sup>5</sup> Consequently, the defect and its associated Frenkel–Poole barrier<sup>19</sup> controls much of the two-terminal response.

In principle, hydrogenation of a defect site and its electronic barrier could make it either more or less transparent to conduction electrons, depending precisely on chemical structure. In practice, every defect prepared via oxidation has exhibited similar conductance *decreases* ( $G/G_0 < 1$ ) when it is probed with H<sub>2</sub>. Furthermore, the responses are uniformly large, order-of-magnitude changes rather than mere 10–50% modulations. While much stronger than the response of defect-free devices, the same mechanism of carrier depletion may still be relevant. The carrier depletion that causes modest responses in diffusive conductors can be greatly amplified at a tunneling or Frenkel–Poole barrier. Because the device resistance depends exponentially on the width of these barriers, a small degree of local carrier depletion that increases the effective width can cause an enormous increase in resistance. Plainly, we interpret the thousand-fold amplification between Figure 1B and Figure 1D to be due to this difference between a diffusive conductor and a Frenkel–Poole or tunneling junction, respectively, and the distinctly different sensitivity each has to local carrier concentration.

**c. Defect Chemistry.** To test whether the chemoresistive response depends on the precise chemistry of the defect site, we have introduced point defects using H<sub>2</sub>O, HNO<sub>3</sub>, HCl, and other solutions as the oxidizing electrolyte.

Figure 2 demonstrates that different defects do indeed have characteristically different response magnitudes after Pd decoration. Oxidation in HCl initially produces –Cl adducts on SWCNT sidewalls,<sup>5</sup> and these defects appear to have the strongest responses and the longest recovery times we have observed. Oxidation by nitric or sulfuric acid, on the other hand, produces weakly scattering epoxide and ether adducts,<sup>5</sup> and these exhibit more modest responses and shorter recovery times. In addition, Figure 2 suggests that the recovery time of different defects might be proportionally related to the logarithm of the chemoresistive

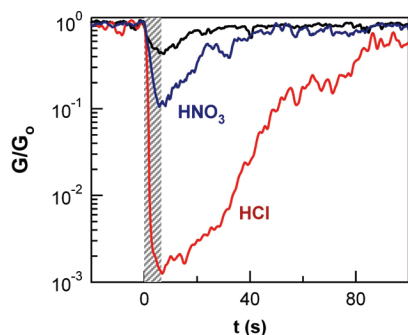


**FIGURE 2.** Comparison of the saturation responses and recovery times of three different, Pd-decorated, SWCNT sensors. High resistance defects from oxidation in HCl give large responses and slow recovery times (red), whereas HNO<sub>3</sub>-induced defects have much smaller responses (blue). Both are compared to the typical response of a semiconducting SWCNT without defects. All three devices include Pd particles, which are necessary for any significant response to occur.

response. Why one type of defect is less responsive than another is an open research question, but relevant theoretical modeling will need to capture chemical interactions between the defect and Pd, H<sub>2</sub>, and atomic H. In any case, different chemical defects are distinguishable experimentally, and dramatically more sensitive than defect-free SWCNTs. This dependence highlights the importance and promise of using different chemical treatments to tailor SWCNT sensors toward particular specifications. However, device responses after such treatments may exhibit long-term drift since some defects are less stable than others against dissociation or other replacement reactions.

**d. Sensitivity at Various Pressures.** Figure 3A depicts the pressure dependence of the resistive response using a defect-free, Pd-decorated s-SWCNT. When no defects are present, the entire chemoresistive effect occurs abruptly around 5 Torr, the pressure at which Pd spontaneously converts to beta phase PdH<sub>x</sub> at room temperature. More modest changes could not be observed using constant pressure soaks performed at pressures above and below the transition point, indicated as vertical bars in the figure. In particular, no measurable response is observable at pressures below a few Torr in this type of defect-free sample.

When a defect is present on the SWCNT, the situation can be very different and the amplified dynamic range of Pd-decorated defects makes it possible to probe much lower H<sub>2</sub> concentrations. For example, Figure 3B depicts the response of two devices exposed to 3 Torr of H<sub>2</sub>.  $G/G_0$  remains close to unity for the defect-free SWCNT, while the SWCNT with a decorated defect decreases toward zero. In the latter case, clear responses can be observed well into the milliTorr range (10–100 ppm H<sub>2</sub>). This experimental range is limited by the exceedingly high resistance of individual, defective SWCNT devices, which at 10 GΩ becomes indistinguishable from the measurement noise floor. In SWCNT films, on the other hand, many parallel conductors contrib-

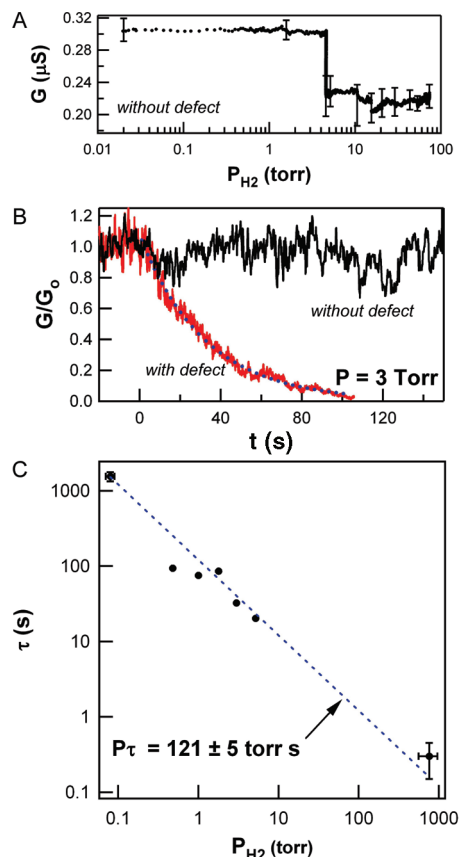


**FIGURE 3.** (A) In the absence of any defects, the response of Pd-decorated SWCNTs is confined to pressures >4 Torr. Measurements of the range of normal device fluctuation are indicated by error bars at the positions of various, fixed pressure soaks. (B) Below 4 Torr, only devices having Pd-decorated defects respond to H<sub>2</sub>. A single exponential fit (dashed line) determines the time constant  $\tau$  at a particular pressure. (C) A single parameter curve fit determines that an inverse relationship exists between pressure and  $\tau$ , indicating that the response is not primarily determined by the total H<sub>2</sub> pressure. Instead, the response is single valued in the H<sub>2</sub> dosage, as defined by the product of  $P$  and  $\tau$ .

ute to a much lower initial resistance and allow for a much wider practical dynamic range. Consequently, film sensors may be more appropriate for testing the ultimate H<sub>2</sub> sensitivity of this defect mechanism. Regardless of the practical sensitivity limit, however, parts A and B of Figure 3 clearly demonstrate that the mechanism at work in SWCNT films, especially in the ppm range, is almost certainly dependent on the contributions of defects.

At low pressures, the measured response time  $\tau$  increases substantially, and Figure 3C demonstrates the relationship between  $\tau$  and  $P$  over the entire experimental range of this report. A curve fit to the raw data determines that the product  $P\tau$  is a constant, with a value  $P\tau = 121 \pm 5$  Torr s for HCl-oxidized SWCNTs. In addition, the saturated total response of a particular defect-containing device is found to be constant, independent of  $P$ , when each experiment is continued long enough to reach equilibrium. We therefore conclude that the integrated H<sub>2</sub> dosage determines  $G/G_0$  and

its rate of change. From this conclusion, the observed decay  $G/G_0 = e^{-t/\tau}$  and the empirically measured  $\tau$  can be directly converted to a simple, pressure-independent expression  $G/G_0 = e^{-N/N_0}$ , where  $N$  is the cumulative dosage of impinging  $H_2$  molecules and  $N_0 = 121 \pm 5 \text{ Torr s} = 1.21 \times 10^8 \text{ langmuirs}$ .

No physical mechanism like charge transfer could reasonably link  $G/G_0$  to such an enormous  $H_2$  dosage, especially since we argue that the response is governed by a single defect site. Alternately, we consider the quantity of atomic H resulting from catalytic dissociation of  $H_2$  on the Pd surface. Pd film experiments measure the sticking and dissociation probabilities of  $H_2$  on Pd to be very high on pristine surfaces in ultrahigh vacuum, but effects such as coadsorption and contamination can limit the same probabilities to 0.2 and  $8 \times 10^{-8}$ , respectively, on films relevant to our ambient conditions.<sup>20–25</sup> With these values, an  $H_2$  impingement dosage  $N_0 = 1.21 \times 10^8 \text{ langmuirs}$  can equal an atomic H dosage  $N_H$  as low as 0.85 langmuirs, or approximately one monolayer of atomic H. The accumulation of this H monolayer on the Pd particle, and the initial spillover of H atoms from the particle onto the defect site, may play the critical role in governing the electronic response. Nevertheless, we note that  $G/G_0$  responses always change continuously in time, rather than via discrete jumps or transitions, proving that the response is sensitive to the entire dosage and not just a single hydrogenation reaction at the defect site.

The conclusion that  $G/G_0$  results from a monolayer dosage of atomic H is appealing because it helps explain multiple features of past experiments. The clear  $\tau$  vs  $P$  dependence observed in vacuum does not occur in air, and this is likely due to competing reactions in air that limit the  $N_H$  dosage to some steady-state equilibrium, even in the presence of excess  $H_2$ . Also,  $G$  does not recover when a device in  $H_2$  is returned to vacuum or inert gas. This feature of SWCNT sensors has been widely reported previously,<sup>2,3</sup> and it indicates that the reverse phase transition of  $PdH_x$  back to Pd has no effect on  $G$ . Instead, recovery with a long  $\tau$  is only enabled when the device is in contact with air, and moist air in particular, implicating one or more slow, chemical processes in the  $G$  recovery mechanism. These experimental features complicate the repeated cycling of single SWCNTs at low pressures, and have severely limited our ability to portray Figure 3C with a more extensive data set. Each test requires venting the test chamber with moist air, recovering high vacuum without moisture, and controlling residual  $H_2$  gas levels despite poor  $H_2$  pumping speeds. During this lengthy process, and perhaps due to other side chemical reactions involved in the recovery, devices can be blown out or otherwise degraded after four to six experimental cycles.

The observed difference in response and recovery times, combined with the lack of recovery when  $H_2$  is removed in vacuum, has complicated efforts to explain the operation of

SWCNT film sensors. H spillover effects, as proposed here, provide a straightforward chemical mechanism for each of these observations. In particular, the asymmetry of hydrogenation and dehydrogenation processes could readily account for differing response and recovery times by the devices.

In conclusion, Pd-decorated defects amplify the chemoresistive response of SWCNT devices to  $H_2$  gas. This amplification results in much better signal-to-noise ratios for sensing experiments, and it is substantially responsible for any detection at all at low  $H_2$  pressures. Whereas defect-free sensing is fixed by the thermodynamics of the Pd– $H_2$  phase diagram, decorated defects are directly sensitive to additional chemical processes including an interaction between the defect and atomic H generated by the Pd. These results provide new insights into the mechanisms of thin film SWCNT sensors, particularly at the lower end of their sensitivity range. The importance of processing and defect concentrations in such films, combined with the opportunities for tailoring these defects, directly impacts the development and application of disordered SWCNT films used as chemical sensors.

**Acknowledgment.** This research was supported by NSF (CBET-0729630, DMR-0936772, and CHE-0802913) and Department of Education GAANN fellowships (V.R.K. and T.S.). Electron microscopy was supported by Carl Zeiss SMT and the Carl Zeiss Center of Excellence at UCI.

**Supporting Information Available.** Nonnormalized resistances, details on the device point oxidation, and other device characteristics. This material is available free of charge via the Internet at <http://pubs.acs.org>.

## REFERENCES AND NOTES

- Zhang, T.; Mubeen, S.; Myung, N. V.; Deshusses, M. A. *Nanotechnology* **2008**, *19*.
- Kong, J.; Chapline, M. G.; Dai, H. J. *Adv. Mater.* **2001**, *13*, 1384.
- Sun, X. Y.; Sun, Y. G. *J. Mater. Sci. Technol.* **2008**, *24*, 569.
- Star, A.; Joshi, V.; Skarupo, S.; Thomas, D.; Gabriel, J. C. P. *J. Phys. Chem. B* **2006**, *110*, 21014.
- Goldsmith, B. R.; Coroneus, J. G.; Khalap, V. R.; Kane, A. A.; Weiss, G. A.; Collins, P. G. *Science* **2007**, *315*, 77.
- Sippel-Oakley, J.; Wang, H. T.; Kang, B. S.; Wu, Z. C.; Ren, F.; Rinzler, A. G.; Pearton, S. J. *Nanotechnology* **2005**, *16*, 2218.
- Robinson, J. A.; Snow, E. S.; Badescu, S. C.; Reinecke, T. L.; Perkins, F. K. *Nano Lett.* **2006**, *6*, 1747.
- Collins, P. G. Defects and disorder in carbon nanotubes. In *Oxford Handbook of Nanoscience and Technology: Frontiers and Advances*; Narlikar, A. V., Fu, Y. Y., Eds.; Oxford University Press: Oxford, 2010.
- An, L.; Owens, J. M.; McNeil, L. E.; Liu, J. *J. Am. Chem. Soc.* **2002**, *124*, 13688.
- Fan, Y.; Goldsmith, B. R.; Collins, P. G. *Nat. Mater.* **2005**, *4*, 906.
- Schlecht, U.; Balasubramanian, K.; Burghard, M.; Kern, K. *Appl. Surf. Sci.* **2007**, *253*, 8394.
- Sayago, I.; Terrado, E.; Aleixandre, M.; Horrillo, M. C.; Fernandez, M. J.; Lozano, J.; Lafuente, E.; Maser, W. K.; Benito, A. M.; Martinez, M. T.; Gutierrez, J.; Munoz, E. *Sens. Actuators, B* **2007**, *122*, 75.
- Heinze, S.; Tersoff, J.; Martel, R.; Derycke, V.; Appenzeller, J.; Avouris, P. *Phys. Rev. Lett.* **2002**, *89*, 162.
- Zhu, W.; Kaxiras, E. *Nano Lett.* **2006**, *6*, 5.

- (15) Chen, Z.; Appenzeller, J.; Knoch, J.; Lim, Y.; Avouris, P. *Nano Lett.* **2005**, *5*, 1497.
- (16) Kim, W.; Javey, A.; Tu, R.; Cao, J.; Wang, Q.; Dai, H. *Appl. Phys. Lett.* **2005**, *87*, 173101.
- (17) Tseng, Y. C.; Phoa, K.; Carlton, D.; Bokor, J. *Nano Lett.* **2006**, *6*, 1364.
- (18) Kauffman, D. R.; Star, A. *Nano Lett.* **2007**, *7*, 1863.
- (19) Mannik, J.; Goldsmith, B. R.; Kane, A.; Collins, P. G. *Phys. Rev. Lett.* **2006**, *97*, 16601.
- (20) Auer, W.; Grabke, H. J. *Ber. Bunsen-Ges.* **1974**, *78*, 58.
- (21) Kay, B. D.; Peden, C. H. F.; Goodman, D. W. *Phys. Rev. B* **1986**, *34*, 817.
- (22) Söderberg, D.; Lundström, I. *Solid State Commun.* **1983**, *45*, 431.
- (23) Rendulic, K. D.; Anger, G.; Winkler, A. *Surf. Sci.* **1989**, *208*, 404.